



## Aerodynamic Characteristics of Multi-Element Iced Airfoil – CFD Simulation

A. Hyll and V. Horák\*

*Department of Mechanical Engineering, Faculty of Military Technology,  
University of Defence, Brno, Czech Republic*

The manuscript was received on 13 September 2012 and was accepted after revision for publication on 20 March 2013.

### **Abstract:**

*The phenomenon of the in-flight icing can affect all types of aircraft. Presence of the ice accretion on wings can lead to performance degradation. Thus, it is important to understand how the different ice shapes affect aerodynamic characteristics. The prediction of the ice accretion on the wing with flaps of different position was made by the in-house code ICE 4.1. The two-dimensional CFD simulation was used for the study of aerodynamic performance degradation of multi-element iced airfoil. The results are discussed and some of them are compared with the wind tunnel testing.*

### **Keywords:**

*Aerodynamics, aircraft icing, performance degradation*

### **1. Introduction**

The in-flight icing, which is a dangerous phenomenon in aviation, can affect all types of aircraft including military aircraft. Icing can adversely affect the flight characteristics of an aircraft. It can increase drag, decrease lift, and cause control problems. The most critical portion of the flight is the landing, when the airplane is flown at slow speeds and low altitudes. A few minutes before landing when flaps are extended the ice accretion on wings and flaps can occur, if the icing conditions are fulfilled. This is the main reason why the decision was made to study the influence of the ice accretion on the wing with flaps. From the aerodynamic viewpoint, when compared to wings without ice, wings with ice indicate decreased maximum lift, increased drag, stall occurring at much lower angles of attack, increased stall speed, and reduced controllability [1]. Thus, it is important to know which ice shapes can be formed on the wings and flaps and understand how they affect the aerodynamics [2].

---

\* Corresponding author: Department of Mechanical Engineering, University of Defence,  
Kounicova 65, 662 10 Brno, Czech Republic, phone: +420 973 442 616, E-mail:  
vladimir.horak@unob.cz

## 2. Simulation of Ice Accretion on Flapped Airfoil

The simulation of the ice accretion on the multi-element airfoil was performed by the in-house code ICE 4.1 [3], which enables to solve a system of several airfoils. This code involves mutual flow overlap of multi-element airfoils (e.g. overlap between the airfoil and flap). The results of air streamlines of droplet trajectories around the airfoil with a slotted flap are shown in Fig. 1. There can be seen droplet trajectories and impact locations near the airfoil leading edge. Trajectories of droplets impacting an airfoil surface are depicted by a black region.

The impact locations, where droplet trajectories intersect an airfoil surface, can be divided into several separated sections. It can be seen for the case of airfoil with extended slotted flap in landing position. The flap is not fully overlapped in this case. Then black regions of impinging droplets trajectories are on both the airfoil leading edge and the flap surface.

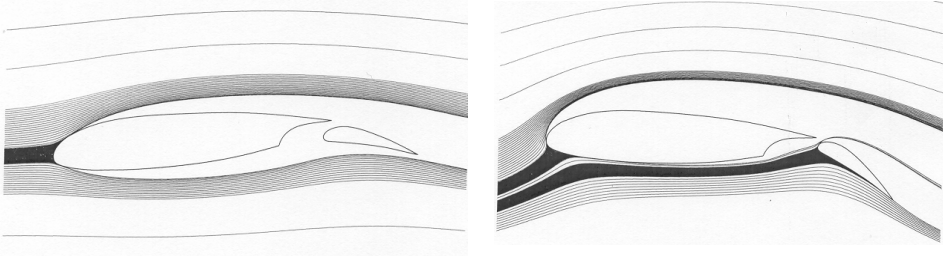


*Fig. 1 Droplet trajectories near the airfoil with a slotted flap and for extended flap in landing position*

The resulting predicted ice shapes on the airfoil with retracted flap position and for angles of deflection  $20^\circ$  and  $38^\circ$  are shown in Fig. 2. The input data of the simulation are: the airfoil chord  $b = 0.6$  m, the free stream velocity  $v_\infty = 42.9$  m s $^{-1}$ , the angle of attack  $\alpha = 0^\circ$ , the cloud liquid water content  $LWC = 0.8$  g m $^{-3}$ , the droplets median volume diameter  $MVD = 15$   $\mu$ m, the ambient air temperature  $T = 273.15$  K, the wing surface temperature  $T_w = 263.15$  K, and the total icing duration time is 600 s.

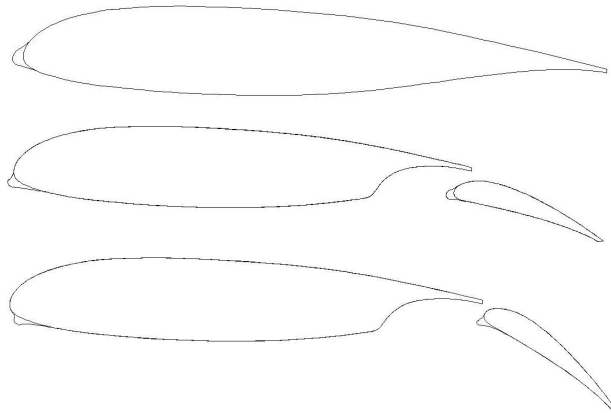


*Fig. 2 Ice prediction on the wing airfoil with a slotted flap: retracted flap and angles of deflection  $20^\circ$  and  $38^\circ$*

The ice accretion on the flap causes reduction of the gap size between main element and flap. Consequently, it can have a large impact on the performance degradation of iced multi-element airfoils. And there is a potential mechanical problem in the elevator mechanism itself as well.

The presented geometry of the iced multi-element airfoils is used for the two-dimensional CFD simulation as the input geometry for the study of the aerodynamic performance degradation.

### 3. Two-Dimensional CFD Simulation

The two-dimensional CFD simulation, based on Reynolds averaged Navier-Stokes equations by the CFD software ANSYS CFX 12.0 [4], was applied to simulate the flow over the shapes of the clean and iced airfoils of retracted flap and for angles of deflection  $20^\circ$  and  $38^\circ$ .

The computational mesh was generated by using the mesh generator ICEM CFD [5]. For computing it was created the hexagonal mesh with the first layer height of  $2 \times 10^{-5}$  m and width varies from  $2 \times 10^{-3}$  m to  $5 \times 10^{-3}$  m, which ensures wall distance  $y^+$  below 3. The elements are growing in the direction of far field. The total number of elements varies from 50000 to 70000 according to the airfoil configuration.

The mesh was smoothed (only for retracted flaps) to ensure a continuous transition between elements. This is important for calculating the transition from laminar to turbulent flow. The grid near the leading edge of the clean airfoil is shown in Fig. 3.

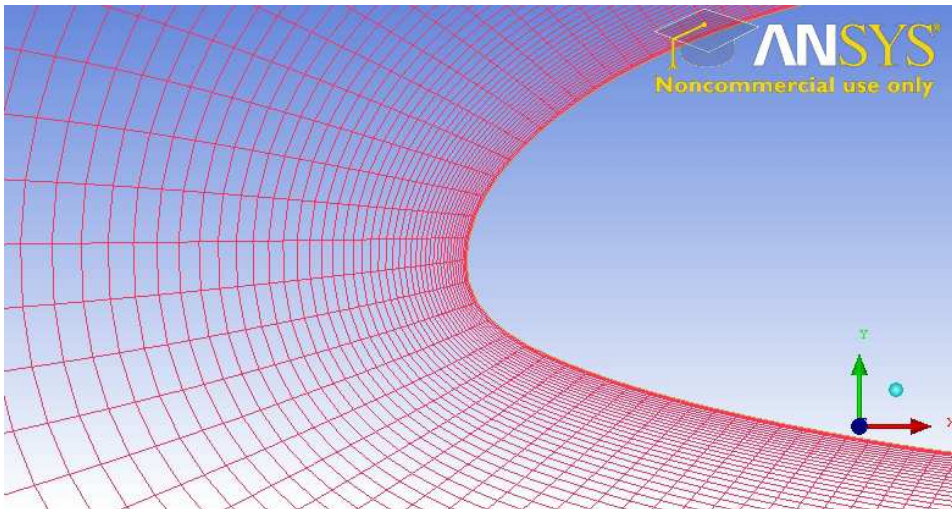


*Fig. 3 Detail of the mesh for clean airfoil*

The input parameters of the CFD simulation were the following:

- The ambient air temperature  $25^\circ\text{C}$
- The incompressible fluid with constant density, with no heat transfer
- The airfoil chord  $b = 0.6$  m

- The free stream velocity  $v_\infty = 44 \text{ m s}^{-1}$
- The Reynolds number corresponding to the given air flow parameters  $Re = 1.75 \times 10^6$
- Low free stream turbulence intensity flow (1 %) was considered
- The used turbulence model is the shear stress transport model and the laminar-turbulent boundary layer transition onset follows gamma-theta model [6], for the profiles with extended flaps the fully turbulent model was chosen to start the simulation and that gamma-theta model was used. Faster convergence was reached by the changing models.
- The calculation was stopped when the average difference between two consecutive matrices (the residual target) reached  $10^{-5}$

The numeric model of ANSYS CFX 12.0 is based on control volume method and iterative solution of resulting system of nonlinear equations [4]. The discretization of geometry is linear and the discretization of solved variables is of second order. The solution is solved as a stationary case. The output of the solution is in the form of 2D display of solved variables in the domain or graph plot of variables along the contour of airfoil.

There are presented some examples of CFX POST outputs for the case of iced airfoil with extended flap of angle of deflection  $20^\circ$  and at the angle of attack  $\alpha = 4^\circ$ . The streamlines around the airfoil are shown in Fig. 4. The density of streamlines is spaced automatically by the ANSYS CFX POST code. Increase in velocity is noticeable above the profiles.

The velocity distribution around the iced airfoil is given in Fig. 5 and Fig. 6.

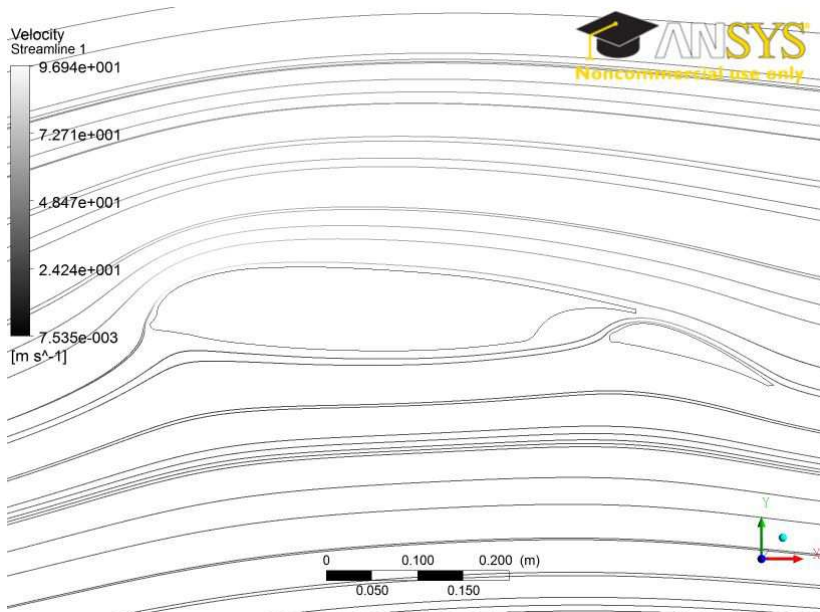


Fig. 4 Streamlines around the iced airfoil

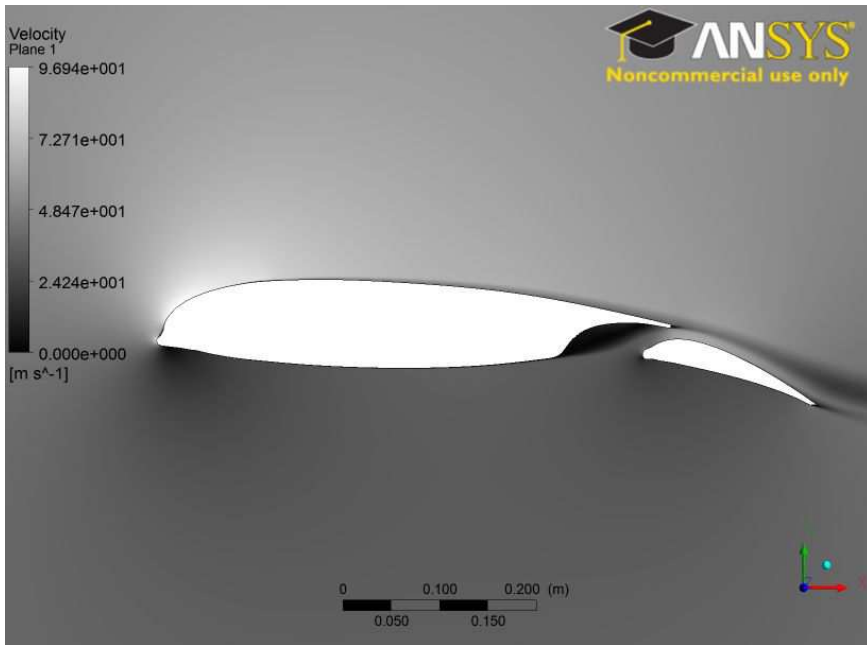


Fig. 5 Velocity distribution around the iced airfoil

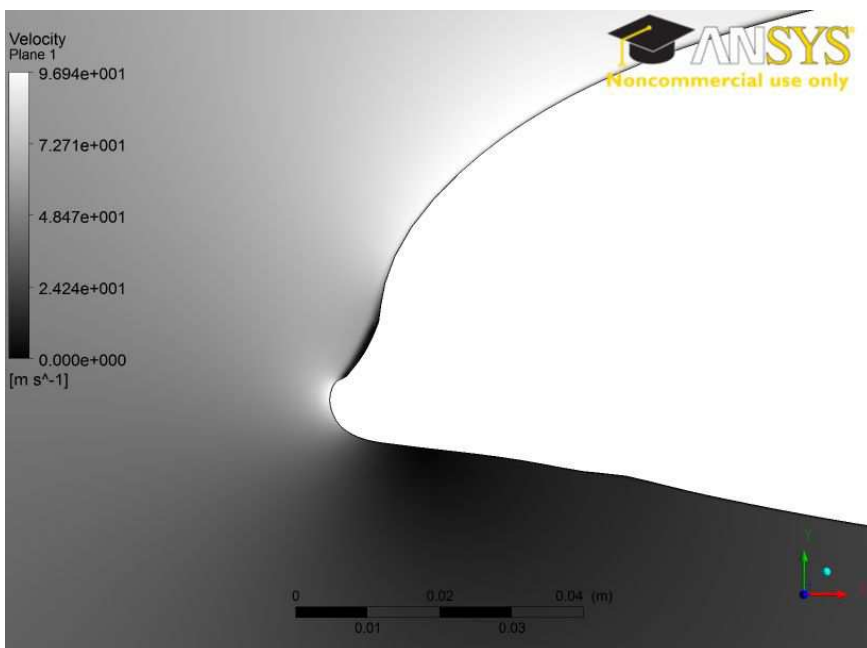
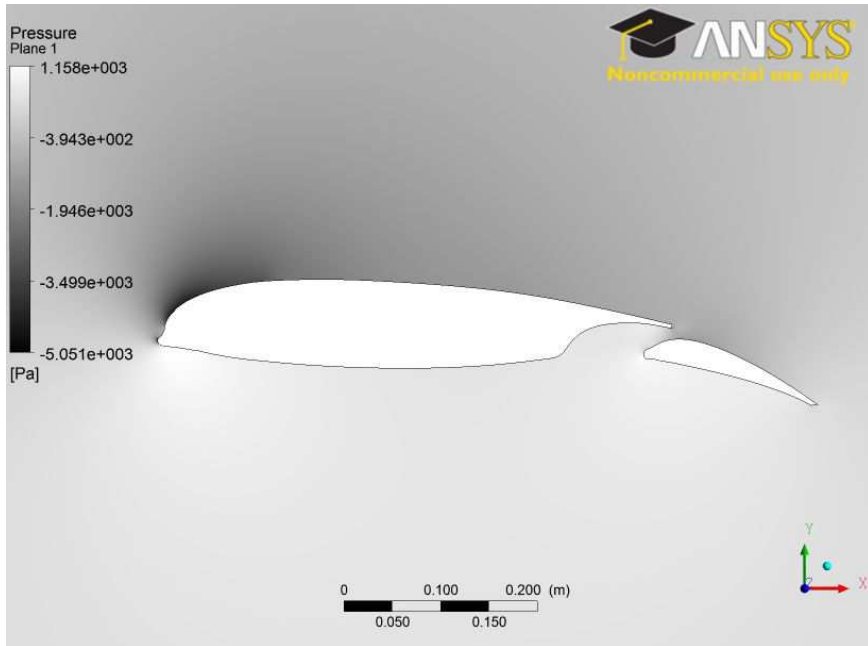


Fig. 6 Velocity distribution near the iced airfoil leading edge

The pressure distribution around the airfoil is an important parameter in terms of integral aerodynamic characteristics. The example of pressure distribution around the iced airfoil with extended flap of angle of deflection  $20^\circ$  and at the angle of attack  $\alpha = 4^\circ$  is given in Fig. 7.



*Fig. 7 Pressure distribution around the iced airfoil*

Pressure on the airfoil surface is automatically integrated along the whole length of the airfoil surface to obtain lift and drag.

#### 4. Presentation of Results and Discussion

The advanced CFD simulation was performed for the flow around the clean flapped airfoil and for the above-mentioned predicted cases of iced airfoils configuration (see Fig. 2). The lift and drag coefficients were obtained by integrating the pressure distribution over the wall along the airfoil surface.

Resulting curves of the lift coefficient  $C_L$  for the clean airfoil with retracted flap and for angles of deflection  $20^\circ$  and  $38^\circ$  at different angles of attack AOA are shown in Fig. 8, where these courses are compared with the wind tunnel experimental data. As can be seen in Fig. 8, the results obtained from the ANSYS CFD simulation agree quite well with the experimental observations.

The results of the CFD simulation as the courses of the lift coefficient for the given cases of iced airfoils (Fig. 2) are presented in Fig. 9 in comparison with the clean airfoil results. It can be seen from this comparison, that the stall occurs at lower angles of attack and the maximum lift is decreased for iced airfoils.

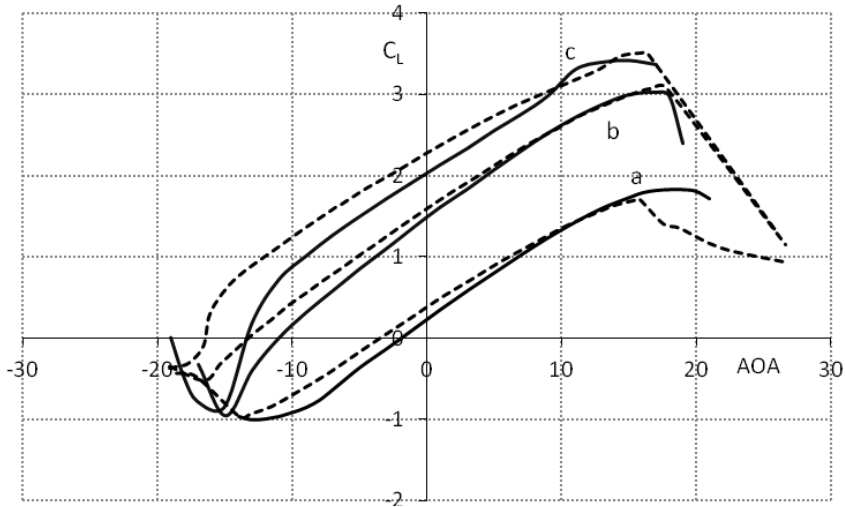


Fig. 8 Comparison of calculated (solid line) and measured (dashed lines) lift coefficients for the clean airfoil for: a) retracted flap; b) angle of deflection 20°; c) angle of deflection 38°

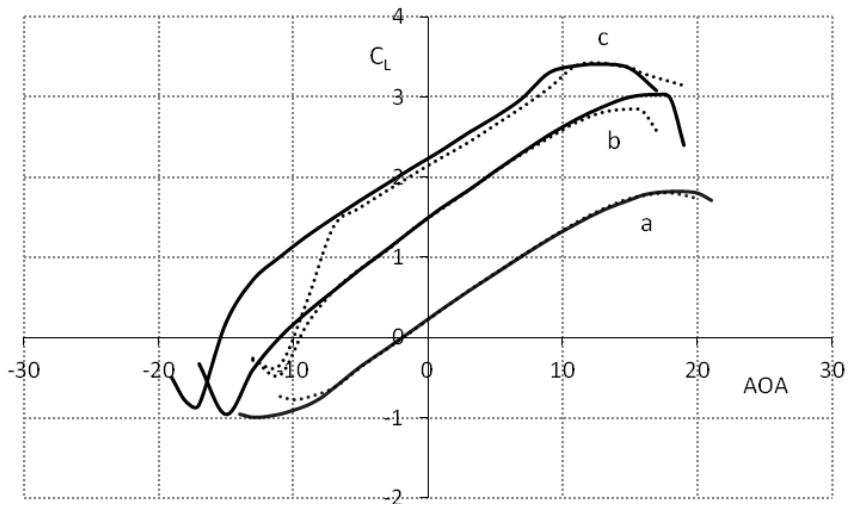


Fig. 9 Comparison of lift curves for clean (solid lines) and iced (dotted lines) airfoils for: a) retracted flap; b) angle of deflection 20°; c) angle of deflection 38°

On the other hand, the computation of the drag coefficients by the CFD simulation usually does not provide us with very good results. Fig. 10 presents the dependence of the drag coefficient  $C_D$  on the angle of attack AOA. It is seen that results of the CFD simulation do not correspond to the wind tunnel testing very well in absolute values, but the curves' tendencies agree with the phenomena.

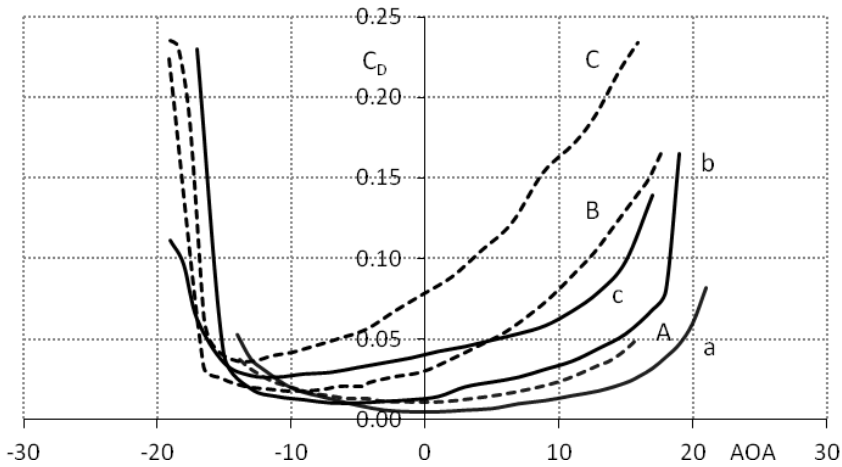


Fig. 10 Comparison of calculated (solid lines, small letters) and measured (dashed lines, capital letters) drag coefficients for: a, A) retracted flap; b, B) angle of deflection 20°; c, C) angle of deflection 38°

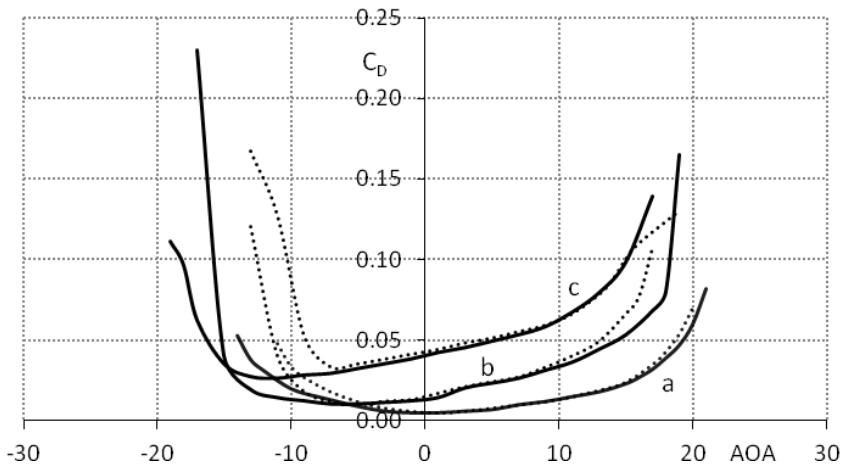


Fig. 11 Comparison of drag curves for clean (solid lines) and iced (dotted lines) airfoils for: a) retracted flap; b) angle of deflection 20°; c) angle of deflection 38°

The results of the CFD simulation as the courses of the drag coefficient for the given cases of iced airfoils are shown in Fig. 11 in comparison with the clean airfoil results. It can be seen the strong influence of icing for negative angles of attack similarly as for lift curves in Fig. 9.

A combined effect of lift and drag is described by the polar curves. Polar curves for clean and iced airfoils for given configurations are shown in Fig. 12.

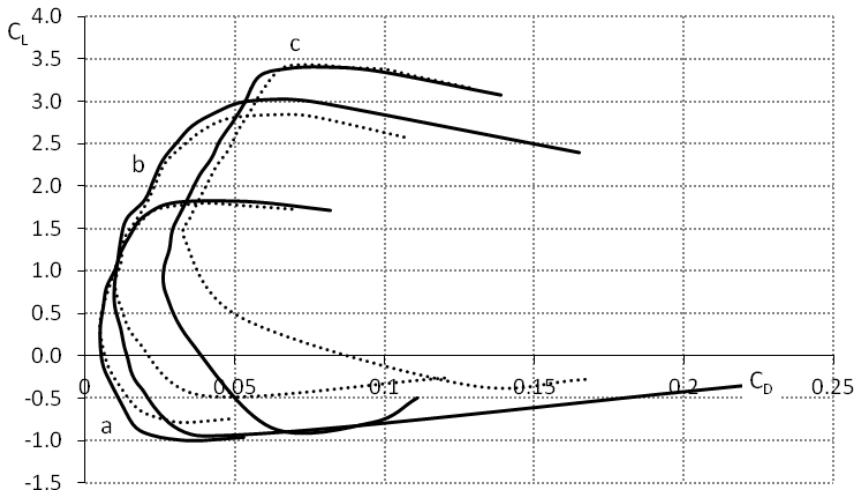


Fig. 12 Comparison of polar curves for clean (solid lines) and iced (dotted lines) airfoils for: a) retracted flap; b) angle of deflection 20°; c) angle of deflection 38°

## 5. Conclusion

The performance degradation of iced airfoils was studied using the CFD simulation. The Navier-Stokes CFD (ANSYS CFX) simulation provides a reasonable prediction of the lift coefficients. Comparing the lift curves for the given multi-element airfoil configurations can result in fairly good agreement between the CFD simulation and wind tunnel testing, as seen in Fig. 8. The CFD prediction of drag coefficient is not so precise (see Fig 10).

The expected stall occurring at lower angle of attack, decreased maximum lift, and increased drag is clearly observable in Fig. 9 and Fig 11, even for this case of relatively low icing. Interesting is the strong influence of icing for the multi-element airfoil, which is observed for negative angles of attack (see Fig. 9 and Fig. 11).

## References

- [1] PARASCHIVOIU, I. and SAEED, F. *Aircraft Icing*. Wiley 1984, 235 p.
- [2] CHÁRA, Z., HORÁK, V. and ROZEHNAL, D. Aerodynamic Degradation of Iced Airfoils – Experiments and CFD Simulations. *Proceedings of the ASME Fluids Engineering Division Summer Conference 2009, FEDSM2009*. Vol. 1, Issue Part C. Vail, Colorado: ASME, August 2-6 2009, p. 1679-1685.
- [3] HOŘENÍ, B., HORÁK, V. and CHÁRA, Z. Improved Ice Accretion Prediction Code. *Advances in Military Technology*, 2008, vol. 3, no. 1, p. 44-50.
- [4] *ANSYS CFX. Reference Guide. Release 12.0*. ANSYS, Inc., April 2009.
- [5] *ANSYS ICEM CFD 11.0. Tutorial Manual*. ANSYS, Inc., January 2007.
- [6] LANGTRY, RB. and MENTER FR. Transition Modeling for General CFD Applications in Aeronautics. *AIAA Paper (2005-522)*, 43<sup>rd</sup> AIAA Aerospace Science Meeting and Exhibit. Reno, Nevada: AIAA, January 2005.

**Acknowledgement**

The work presented in this paper has been supported by the Czech Science Foundation project No. P101/10/0257 and by the institutional development funding PRO-K216 “Support of Research, Experimental Development, and Innovation in Mechanical Engineering”.